Explanation of Worksheets for
Chapter 9 (Climate and Climate-System Modelling) of the textbook

"Environmental Modelling: Finding Simplicity in Complexity, 2nd Edition"

edited by John Wainwright and Mark Mulligan,
to be published by Wiley-Blackwell in early 2011

L. D. Danny Harvey
Department of Geography
University of Toronto
100 St George St
Toronto, Canada M5S 3G3

harvey@geog.utoronto

DRAFT TEXT (29 June 2010) – COMMENTS ARE WELCOME

Overview

The online material consists of an Excel file with worksheets that fall into two groups: Part 1 (Worksheets 1 to 7), which illustrates basic features of simple climate models and of models of the terrestrial biosphere component of the carbon cycle, and Part 2 (Worksheets 8 to 18), which contains worksheets for generating scenarios of future CO_2 emissions, then computing the buildup of atmospheric CO_2, the climate response, and feedbacks between climate and the carbon cycle. The CO_2 emissions are generated as the result of specific assumptions concerning population, economic growth, decreasing energy intensity (MJ per $ of GDP), and the rate of deployment of C-free energy supplies. Those interested only in exploring the climatic consequences of alternative assumptions in these areas should jump directly to Worksheet 8.

PART 1: Climate and Terrestrial Biosphere Model Basics

Worksheet 1   Zero-dimensional model with no atmosphere

The Earth's temperature is governed by the balance between the rate of absorption of solar radiation and the rate of emission of infrared radiation to space. Absorption of solar radiation has a warming effect, while emission of infrared radiation has a cooling effect. An increase in temperature leads to an increase in the emission of infrared radiation. The difference between the two (absorbed solar minus emitted infrared radiation) is referred to as the *net* radiation. If the net radiation is positive, the climate warms, but this warming leads to an increase in emission of infrared radiation, thereby eventually reducing the net radiation to zero, at which point no further change in temperature will occur. Similarly, if the net radiation is negative, temperature decreases, which reduces the emission of infrared radiation and eventually increasing the net radiation to zero.

The average intensity of solar radiation (W/m^2) on a plane perpendicular to the Sun's rays at the mean Earth-Sun distance is referred to as the *solar constant* (Q_s). The amount solar radiation intercepted by the Earth is equal to the solar constant times the area of the 2-dimensional disc of the Earth as seen from the sun, namely, $Q_s \pi R_e^2$, where R_e is the radius of the Earth. The surface area of the Earth is $4\pi R_e^2$, so the intercepted solar flux averaged over the entire Earth is simply $Q_s/4$. This is the average global solar radiation flux incident on a horizontal plane above the atmosphere. The fraction of solar radiation arriving at the top of the atmosphere that is ultimately reflected back to space is referred to as the *planetary albedo* (α_p).

The maximum possible rate of emission of radiation (W/m^2) by a body at temperature T is equal to σT^4, where σ is the Stefan-Boltzman constant. An object that emits at the maximum possible rate is referred to as a *blackbody*. The Earth's surface and clouds emit infrared radiation very closely to the backbody rate, but at different temperatures. Some of this radiation is absorbed within the atmosphere, which in turn emits its own radiation, but not as a blackbody. Let F be the observed overall emission of infrared radiation to space from the Earth. We can define the *effective* radiating temperature of the Earth as the temperature of a blackbody that would emit the same amount of radiation as the actual amount of radiation F seen from space. That is, $\sigma (T_{eff})^4 = F$, so $T_{eff} = (F/\sigma)^{0.25}$.

With this background, we can write an equation governing the average effective radiating temperature of the Earth, namely,

$$(1-\alpha_p)\frac{Q_s}{4} - \sigma T_{\textit{eff}}^4 = N(T_{\textit{eff}}) = 0 \tag{1}$$

where the first term on the left hand side is the global mean rate of absorption of solar radiation and the second term is the rate of emission of infrared radiation. The difference between the two is the net radiation N and is a function of the effective radiating temperature. Equation (1) is a zero-dimensional climate model, as it represents the Earth as a single point with a single temperature. Although we're treating the Earth as a single point (that is, with no variation east-west, north-south, or vertically), we use as the average solar flux incident on the Earth the average flux on the real, spherical Earth.

If a radiative perturbation ΔR is imposed that is independent of the radiating temperature, the new energy balance equation is

$$(1-\alpha_p)\frac{Q_s}{4} + \Delta R - \sigma T_{\textit{eff}}^4 = N(T_{\textit{eff}}) + \Delta R = 0 \tag{2}$$

where positive ΔR means a net heating effect, either through an imposed increase in the absorption of solar radiation or an imposed decrease in the emission of infrared radiation to space. Both Eq. (1) and (2) can be solved algebraically for $T_{\textit{eff}}$, as shown in the worksheet, but we can use this model to illustrate in iterative solution technique as well.

Let T_1 be the temperature that satisfies Eq. (1) (having no radiative perturbation) and T_2 the temperature that satisfies Eq. (2). Furthermore, write T_2 as $T_2 = T_1 + \Delta T$. Then $N(T_2) \sim N(T_1) + (dN/dT)\Delta T$ (this is a first-order Taylor Series Expansion) and

$$N(T_2) + \Delta R = N(T_1) + (dN/dT)\Delta T + \Delta R = 0 \tag{3}$$

But $N(T_1) = 0$ by definition, so we get

$$\Delta T = -\frac{\Delta R}{dN/dT} \tag{4}$$

where $dN/dT = -4\sigma T^3$. When T_2 calculated in this way is substituted into Eq (2), we find that $N(T_2) + \Delta R$ is not exactly zero (the reason being that we have implicitly extrapolated a constant dN/dT over the temperature interval ΔT, whereas dN/dT changes continuously with temperature). The imbalance can be treated as a radiative perturbation that can be used in Eq. (4) to compute an additional ΔT that is added to the original ΔT. This process is repeated until the additional ΔT is negligibly small, as illustrated in the worksheet.

Worksheet 2   Zero-dimensional model with atmosphere and atmospheric feedbacks

The Earth does not in reality emit radiation to space as a blackbody (not even as a blackbody at the effective radiating temperature). However, the emission to space is still some function of T. Similarly, the absorption of solar radiation is some function of T. The energy balance equation can be written as

$N(T)=Q(T)-F(T)=0$ (5)

where $Q(T)=(1-\alpha_p(T))Q_s/4$ is the global mean rate of absorption of solar radiation and $F(T)$ is the global mean rate of emission of infrared radiation to space. Eq. (4) is still applicable and $dN/dT=dQ/dT-dF/dT$. Thus,

$$\Delta T = -\left(\frac{\Delta R}{dQ/dT - dF/dT}\right) = \frac{\Delta R}{dF/dT - dQ/dT}$$ (6)

where dF/dT and dQ/dT can be expanded as

$$\frac{dF}{dT} = \frac{\partial F}{\partial T} + \sum_{i=1}^{n} \frac{\partial F}{\partial I_i} \frac{dI_i}{dT}$$ (7)

and

$$\frac{dQ}{dT} = \sum_{i=1}^{n} \frac{\partial Q}{\partial I_i} \frac{dI_i}{dT}$$ (8)

respectively.

The total derivative dF/dT involves the dependence of F on temperature in two ways: a direct dependence on temperature ($\delta F/\delta T$), and an indirect dependence on temperature through the direct dependence of F on various internal variables I_i ($\delta F/\delta I$) which in turn directly depend on temperature (dI_i/dT). An example of an internal variable on which F depends is the amount of water vapour in the atmosphere. As noted in the discussion of Worksheet 1, the maximum possible rate of emission of radiation is the blackbody emission, $F_{max} = \sigma T^4$. This expression arises as the integral (summation) over all wavelengths of an expression called the *Planck function*. The emission to space can be represented as $F = \sigma(T_{eff})^4$, so $\delta F/\delta T = 4\sigma(T_{eff})^3$; that is, $\delta F/\delta T$ is the derivative of the Planck function or blackbody emission evaluated at the effective radiating temperature of the Earth. Q depends on many individual variables, such as cloud amounts and cloud optical properties, and atmospheric and surface reflectivity, all of which change with temperature, but does not depend directly on temperature (so there is no $\delta Q/\delta T$ term in Eq. (8)).

A negative feedback corresponds to $dN/dT < 0$, and the overall feedback is negative; that is, as the temperature increases in response to an initial surplus of radiation, the net radiation decreases, which limits the subsequent temperature increase. As $N(T)=Q(T)-F(T)$, the total derivative dN/dT can be written as

$$\frac{dN}{dT} = \frac{\partial N}{\partial T} + \sum_{i=i}^{n} \frac{\partial N}{\partial I_i} \frac{dI_i}{dT}$$ (9)

with $\delta N/\delta T = -\delta F/\delta T$ and $\delta N/\delta I = \delta Q/\delta I - \delta F/\delta I$. The term $\delta N/\delta I_i \, dI_i/dT$ represents the inherent strength of a given feedback process i. As a more negative dN/dT represents a stronger negative feedback, $\delta N/\delta I_i \, dI_i/dT < 0$ represents a negative feedback and $\delta N/\delta I_i \, dI_i/dT > 0$ represents a positive feedback.

Because $N(T)=Q(T)-F(T)$ and $dN/dT < 0$ is a negative feedback, it can be seen that stronger dF/dT (that is, a more rapid increase in the emission of infrared radiative to space as the planet warms) results in a stronger negative feedback, and hence a smaller warming. This is also clear from Eq. (6): a larger dF/dT results in a smaller ΔT. The single largest factor contributing to this overall negative feedback is the increase in emission through the Planck function, $F = \sigma T^4$, such that $\delta F/\delta T = 4\sigma T^3 = 3.76$ W/m²/K.

Conversely, if the absorption of solar radiation increases as the climate gets warmer (that is, if $dQ/dT > 0$), this constitutes a positive feedback. An increase in absorption of solar energy means a decrease in the reflection of solar energy to space, that is, a decrease in the planetary albedo α_p. The global mean absorption of solar radiation is equal to $(1- \alpha_p)Q_s/4$, so $\delta Q/\delta\alpha_p = -Q_s/4$ and $dQ/dT=-(Q_s/4)\, d\alpha_p/dT$. Thus, if the planetary albedo decreases as T increases (which would normally be the case), then $dQ/dT>0$, which increases ΔT (as seen from Eq. (6)).

The climate sensitivity is defined as the longterm (or "equilibrium") temperature response to a doubling of the atmospheric CO_2 concentration (for which $\Delta R=3.75$ W/m²). Table 1 in the spreadsheet, reproduced below, gives low and high estimates of the sizes of various terms that contribute to dN/dT, and the resulting climate sensitivity.

Table 1, Worksheet 2 Hypothetical combination of feedbacks giving low and high climate sensitivity. Given is $\delta N/\delta I_i\, dI_i/dT$ for each listed internal variable i. The overall feedback is negative (due to the dominance of the Plank function term), but the net effect of the remaining feedbacks is either weakly or strongly positive.

Feedback	$\delta N/\delta I_i\, dI_i/dT$ (W/m²/K)	
	Weak positive feedback exclusive of the Planck function	Strong positive feedback exclusive of the Planck function
Planck function	-3.76	-3.76
water vapour, IR effect	1.50	2.50
water vapour, solar effect	0.20	0.20
lapse rate	-0.30	-0.70
clouds - IR effect	-0.80	1.20
clouds - solar effect	0.50	-0.50
surface albedo	0.20	0.23
Non-Plank function feedback	1.30	2.93
dN/dT	-2.46	-0.83
Climate sensitivity	1.52	4.51

Table 2 from the worksheet illustrates the fact that adding a positive feedback of a given strength has a larger impact on the climate sensitivity the larger the pre-existing climate sensitivity. From Eq (4) it can be seen that the smaller $-dN/dT$ is, the greater the impact on climate sensitivity of adding a given additional small positive feedback (that is, the greater the impact of making $-dN/dT$ smaller still by a given amount). This illustrates a very important point: a given additional positive feedback has a greater effect on climate sensitivity the greater the strength of the pre-existing positive feedbacks (or the greater the pre-existing climate sensitivity).

Table 2, Worksheet 2 Illustration of how the effect on climate sensitivity of adding a feedback with a given strength depends on the pre-existing climate sensitivity		
Initial dN/dT (W/m^2/K)	-2.46	-0.83
Initial climate sensitivity (K)	1.52	4.51
Additional small feedback (W/m^2/K)	0.2	0.2
New dN/dT (W/m^2/K)	-2.26	-0.63
New climate sensitivity (K)	1.66	5.95
Impact on ΔT (K)	0.13	1.43

Worksheet 3   Linear feedback analysis

Consider the case where there are no feedbacks except through the direct dependence of infrared emission on temperature (so $dF/dT = \partial F/\partial T$ and $dQ/dT=0$). With ΔR equal to the radiative forcing, the temperature response ΔT can be written as

$$\Delta T = G_o \Delta R \tag{10}$$

where G_0 is referred to as the *system gain*. By comparison of Eq. (10) with Eq. (6), we see that $G_0=(\partial F/\partial T)^{-1}$. When indirect feedbacks are allowed, the change in temperature leads to a further change, ΔJ, in the net radiation, which then feeds back into the system, as shown in **Figure 1.**
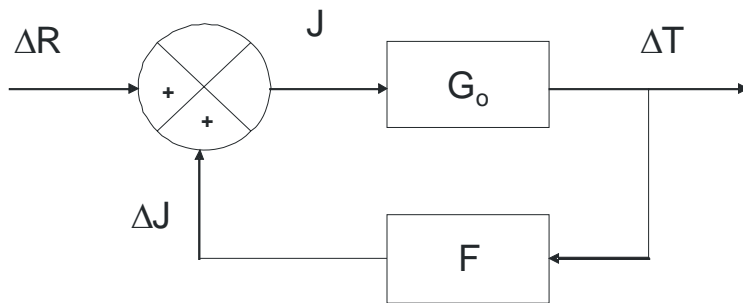

Figure 1: Block diagram show a climate feedback loop.

The temperature response is now given by

$$\Delta T = G_o(\Delta R + \Delta J) \tag{11}$$

On the assumption that the individual feedbacks are independent of one another, then $\Delta J=\Sigma \Delta J_i$, where each ΔJ_i is the change in net radiation due to the change in ΔT provoking feedback process i. It can be written as

$$\Delta J_i = \left(\frac{\partial Q}{\partial I_i} - \frac{\partial F}{\partial I_i} \right) \frac{dI_i}{dT} \Delta T = \frac{\partial N_i}{\partial I_i} \frac{dI_i}{dT} \Delta T \tag{12}$$

where $N=Q-F$ is the net radiation at, strictly speaking, the tropopause. If ΔR and ΔJ_i are both positive or both negative, then the feedback involving variable i is a positive feedback since it reinforces the initial heating perturbation. Alternatively, we can write the ΔJ_i as $\Delta J_i = G_i \Delta T$. Letting $G = \Sigma G_i$, we can rewrite Eq. (12) as

$$\Delta T = G_o (\Delta R + G \Delta T) \tag{13}$$

Solving for ΔT, we obtain

$$\Delta T = \left(\frac{G_o}{1-f} \right) \Delta R \tag{14}$$

where $f = G G_0 = \Sigma f_i$, and

$$f_i = G_o \frac{\partial N}{\partial I_i} \frac{dI_i}{dT} = G_o \frac{\Delta J_i}{\Delta T} \tag{15}$$

The variables f and f_i are referred to as the *feedback factor*. The magnitude of f_i is a measure of the strength of the feedback involving variable i; it is positive for a positive feedback and negative for a negative feedback. The ratio of ΔT with all feedbacks to ΔT without indirect feedbacks, R_f, is equal to $1/(1-f)$. The figure embedded in Worksheet 3 shows the warming for a CO_2 doubling as a function of f. In deriving the results leading up to this figure, we have assumed that (i) the strength of each feedback is independent of all the other feedbacks, and (ii) the strength of the feedback does not change as the magnitude or sign of ΔR and ΔT changes. In other words, we have assumed that the system is *linear*. Nevertheless, the increase in ΔT with increasing f (as more positive feedbacks are added) is decidedly nonlinear: a given increase in f has a greater absolute effect on ΔT the greater the initial value of f. Thus, the effect of a given feedback on ΔT depends on what other feedbacks are already present – a result demonstrated already in Worksheet 2. Another important lesson that can be drawn from this analysis is that an infinitely strong negative feedback cannot reverse the sign of the temperature response, but rather, drives the response to zero.

The assumption of constant and independent feedbacks has been evaluated by Schlesinger (1985) and is a reasonably valid approximation except when combining multiple feedbacks involving clouds (such as cloud amount and cloud optical depth), in which there are important interactions between the feedbacks. However, this does not invalidate the important insights that we have derived from the analysis here.

Finally, it should be noted that the feedback factors associated with individual feedback processes in a complex climate model (such as a 3-D atmospheric general circulation model (AGCM)) can be directly computed from the equilibrium changes produced by a climate model. To do so, one would first compute the global mean net radiation over the course of one year associated with the equilibrium (unchanging) climate prior to applying a radiative forcing (such as imposing an increase in atmospheric CO_2). To compute the feedback factor associated with water vapour changes, for example, one would then repeat the calculation of annual net radiation using the new water vapour amounts produced after a new equilibrium had been reached following a CO_2 increase (or other

forcing), but using the original values for all other variables including temperature. The difference in net radiation gives ΔJ_i. This divided by the global mean change in surface temperature associated with the altered water vapour amounts and times G_o gives the f_i for water vapour. ΔJ_i divided by ΔT alone gives the product $\delta N/\delta I_i \, dI_i/dT$, which is given in Table 1 for hypothetical strong and weak feedback cases. Examples of calculations of the product $\delta N/\delta I_i \, dI_i/dT$ from recent AGCMs can be found in Bony et al. (2006, Fig. 1) and Ringer et al. (2006, Fig. 2).

Worksheet 4   Linear feedback analysis with climate-carbon cycle feedbacks

In Worksheet 3, the system gain and the feedback factor f have been directly specified. This feedback factor and the associated climate sensitivity take into account so called 'fast' feedback processes – things such as the retreat of seasonal land snow cover and sea ice, changes in the amounts and properties of clouds, and changes in the amount of water vapour in the atmosphere. The climate sensitivity is defined as the equilibrium response for a fixed increase in CO_2 concentration (namely, a doubling), but once the climate begins to warm, the CO_2 (and also the methane (CH_4)) concentration would change further due to changes in the natural fluxes of CO_2 (and CH_4) into and out of the atmosphere. However, most of these processes would unfold slowly as the climate warms and tend to cause further warming (a positive feedback). Reductions in the extent of glacier ice caps and changes in the geographical distribution of different biomes (which differ in their reflectivity to solar radiation) would also unfold slowly but exert a positive feedback on the initial climatic change. These are therefore referred to as 'slow' feedback processes. We can thus think of two different climate sensitivities – one based on fast feedback processes and assuming fixed GHG concentrations, and the other taking into account slow feedback processes and changes in greenhouse gas concentrations themselves.

The slow feedback processes involving the carbon cycle can be represented through an additional feedback factor f_{cc}. Simulations with detailed models of the carbon cycle indicate that the net feedback between climate and the carbon cycle is positive, that is, that an increase in temperature leads to an increase in the atmospheric CO_2 concentration, which induces a further increase in temperature. Experiments with a variety of earth-system models of intermediate complexity by Plattner et al. (2008) indicate that, for most models, the amount of carbon stored in the terrestrial biosphere and oceans decreases by 40-80 Gt and 10-30 Gt, respectively, per Celsius degree of warming. These correspond to dC/dT of 20-40 ppmv/K and 5-15 ppmv/K, respectively.

Here, the carbon cycle feedback factor f_{cc} is computed as follows: (1) a rate of increase in the steady state atmospheric CO_2 concentration with temperature, dC/dT, is specified; (2) $\partial N/\partial C$ is estimated from the equation for the radiative forcing due to CO_2,

$$\Delta R = \Delta R_{2x} \frac{\ln(C/C_o)}{\ln 2} \tag{16}$$

where R_{2x} is the forcing for a CO_2 doubling (3.75 W/m^2), C is the current CO_2 concentration, and C_o is the initial CO_2 concentration (280 ppmv); and (3) f_{cc} is computed using Eq. (15). From Eq (16) it follows that

$$\frac{\partial N}{\partial C} = \left(\frac{\Delta R_{2x}}{\ln(2)} \right) \frac{1}{C} \tag{17}$$

f_{cc} is then added to the previous f to get a new total f, which is then used in Eq. (14) to estimate the temperature change when both climate (fast) feedbacks and climate-carbon cycle feedbacks are included. An example is given in Worksheet 4. The accuracy of this approach is evaluated by comparing the estimated ΔT with that computed from an iterative application of the fast and slow feedback processes: an initial CO_2 increase is specified, the initial radiative forcing is computed, an initial ΔT is computed using the feedback factor f for fast feedback processes, the additional increase in CO_2 concentration due to the initial warming is computed using the initial ΔT and the specified dC/dT, a new CO_2 concentration and radiative forcing are computed, and a new estimate of ΔT is computed using the new radiative forcing but the original fast feedback factor. The revised warming leads to a further increase in CO_2 concentration, so the process is repeated until there is almost no further calculated warming or increase in CO_2 concentration. For f=0.5 (corresponding to a climate sensitivity of 2.0 K), $dC/dT = 20$ ppmv/K and an initial increase in CO_2 concentration from 280 ppmb to 560 ppmv, f_{cc} as computed from Eqs. (15) and (17) is equal to 0.06394 and the estimated ΔT estimated using Eq. (15) (that is, using the linear feedback analysis) is 2.230 K, an enhancement of 15% compared to the 1.994 K warming that would occur if the CO_2 concentration remained fixed at 560 ppmv. The final warming as computed with the iterative procedure is 2.213 K, an enhancement of only 11%. However, the error in the final warming using the f_{cc} approach is only 3.3%, which is far less than the uncertainty than in either the climate sensitivity or in the strength of the climate-carbon cycle feedback. When f=0.75 (giving a climate sensitivity of 4.0 K, then the two estimates of the temperature change after climate-carbon cycle feedbacks are 5.36 K and 4.92 K - an error 8.9%. When f=0.75 and $dC/dT = 40$ ppmv/K, the error grows to 35%. The linear feedback approach always overestimates the final warming because the decrease in $\partial N/\partial C$ as the warming grows, due to the dependence of the radiative forcing due to increasing CO_2 on the logarithm of the CO_2 concentration, is not accounted for in the linear feedback analysis.

It is instructive to compare the relative enhancement in the warming as a result of the climate-carbon cycle feedback for different initial CO_2 perturbations, climate sensitivities, and CO_2 sensitivities (dC/dT). This is left as an exercise for the reader.

Worksheet 5   One-box, time-dependent climate model

The previous worksheets calculate the change in planetary temperature required to re-establish zero net radiation after imposing a radiative perturbation, what climate scientists call the "equilibrium" climate or temperature change. In reality, there would be a gradual approach to the equilibrium temperature change rather than an instantaneous response, due to the fact that the atmosphere, land surface layer, and oceans all have a non-zero heat capacity. The time dependent response is referred to as the *transient* temperature response. Worksheet 5 presents the transient response for the simplest possible case, in which only a single temperature is computed, which can be thought of as representing a single box. This box represents some combination of the atmosphere, land surface and upper layer of the ocean.

The upper layer of the ocean is referred to as the *mixed layer* because it is vigorously mixed by wind action, and so – at any given location – has a rather uniform temperature. A typical depth of this layer is about 70 m. Over land, a layer only a few meters in thickness will appreciably heat up or cool down over a time scale of years.

As before, we consider the average energy balance per m^2 of horizontal surface area. The heat capacity of the atmosphere, land surface and upper layer of the ocean can be represented by the heat capacity of a single layer of water of depth h. The product $I=\rho c_p h$, where ρ is the density of seawater (1027 kg/m^3) and c_p is the specific heat of water (4.186 x 10^3 J/kg/K), is referred to as the

thermal inertia of the layer. It gives the amount of heat required per square metre of horizontal area to raise the temperature of the box by 1 K. A simple approach is to use for h the area-weighted average of the mixed layer depth (70 m) and the depth of water having the same thermal inertia as the land surface (about 2 m), namely, h=50 m (as discussed by Thompson and Schneider (1979), the harmonic mean of the two depths is more appropriate). This gives $I = 2.1$ x 10^8 J/m²/K. Changes in temperature are governed by

$$I\frac{dT}{dt} = Q - F \tag{18}$$

where, as before, Q is the global mean absorption of solar radiation and F is the emission of infrared radiation to space. If the planet is initially in a balanced state (Q=F), and a radiative forcing of magnitude ΔR is applied, the equation governing the change in temperature, ΔT, is

$$I\frac{d\Delta T}{dt} + \lambda\Delta T = \Delta R \tag{19}$$

where $\lambda = $ dF/dT-dQ/dT is the *radiative damping parameter* (it is the negative of dN/dT, which was considered in the previous worksheets). A larger λ means that the net radiative *loss* increases more strongly with increasing temperature, which limits the final temperature increase (that is, it makes the climate sensitivity smaller). The solution to Eq. (19) is

$$\Delta T(t) = \Delta T_{eq}(1 - e^{-t/\tau}) \tag{20}$$

where ΔT_{eq} is the equilibrium temperature change, and τ=I/λ. ΔT_{eq} is given by

$$\Delta T_{eq} = \Delta R / \lambda \tag{21}$$

A detailed derivation of Eqs. (19) and (20) is presented in **Box 1**. When t=τ, the temperature has changed by 1-e^{-1}=0.632 of the final change, when t=2τ the temperature warms by another 0.632 of the change that still had to occur at t=τ, and so on, as ΔT asymptotically approaches ΔT_{eq}. τ is referred to as the *e-folding* time, and it depends on the thermal inertia *and* the radiative damping parameter. For a 70 m deep mixed layer and $\lambda = 2$ W/m²/K (corresponding to about 2 K warming for a CO_2 doubling), $\tau \approx 3.5$ years. The transient response of the one-box model is illustrated in the figure that is embedded in Worksheet 5.

Since ΔT_{eq}=ΔR/λ and τ=I/λ, it immediately follows that τ varies in direct proportion to the climate sensitivity. Thus, if the assumed climate sensitivity is larger, the ultimate climatic change will be larger, but the approach to the final climatic change will be slower in relative terms. These differences will have competing effects on the absolute temperature change that occurs during the initial response. Users of Worksheet 5 can explore these relationships themselves. The net result is that there is relatively little difference in the absolute temperature increase during the early part of the transient for trajectories that are ultimately heading to quite different final temperature changes. This makes it difficult to constrain the climate sensitivity from observations during the early part of a transient response.

If we were to consider the atmosphere rather than the mixed layer as a single, well-mixed box, then $\tau \approx 4$ months, since R for the atmosphere is about 1 x 10^7 J/m²/K instead of 3 x 10^8 J/m²/K. However, the atmosphere and mixed layer are so tightly coupled through sensible and latent heat

exchanges that the atmosphere cannot warm significantly faster than the mixed layer without creating a large counteracting heat flux between the two (as demonstrated in Harvey, 2000, Box 3.3); thus, the atmosphere and mixed layer warm together with a time constant governed by the mixed layer thermal inertia. The same applies to the difference between the atmosphere and land surface. Thus, we are justified in considering a single box to represent the combination of the atmosphere, land surface and mixed layer.

To implement Eq. (18) in the Excel worksheet we need to specify Q and F as a function of T. The Planck function ($F = \sigma T^4$) is not applicable to a planet with an atmosphere and where water vapour content increases with temperature. Rather, we will represent outgoing radiation, as well as the planetary albedo, as linear functions of temperature:

$$F = A + BT \tag{22}$$

$$\alpha_p = a + bT \tag{23}$$

Then,

$$\lambda = B + b\frac{Q_s}{4} \tag{24}$$

The model can be adjusted to have any desired climate sensitivity. If b is fixed at, say, 0.001/K, then B can be chosen to produce the λ that produces the desired ΔT_{eq} through Eq. (21). A can then be chosen to give the observed outgoing infrared emission of about 240 W/m^2 when the calculated temperature is equal to the observed global mean surface air temperature of about 289 K.

Box 1:   Derivation of Equations 19 and 20

The governing equation for a planet consisting of a single mixed layer with temperature T is

$$I\frac{dT}{dt} = Q - F \tag{B1}$$

Rather than dealing with the above equation, involving the total temperature T and total radiative fluxes, it is much more convenient to deal with temperature and radiative flux perturbations. To derive an equation governing temperature perturbations, we write

$$T = T_o + \Delta T \tag{B2}$$

$$Q = Q_o + \frac{dQ}{dT}\Delta T \tag{B3}$$

$$F = F_o + \frac{dF}{dT}\Delta T \tag{B4}$$

where T_o is the steady-state temperature and Q_o and F_o are the corresponding radiative fluxes. The temperature perturbation from the initial steady state, ΔT, arises in response to some external

forcing ΔR. Adding ΔR to the right hand side of Eq. (B1) and substituting Eqs. (B2) to (B4) into Eq. (B1), we obtain

$$I\frac{d(T_o + \Delta T)}{dt} = \left(Q_o + \frac{dQ}{dT}\Delta T\right) - \left(F_o + \frac{dF}{dT}\Delta T\right) + \Delta R \qquad (B5)$$

However, dT_o/dt and $Q_o - F_o$ equal zero (by the definition of steady state), so these terms can be subtracted from Eq. (B5) to yield

$$I\frac{d\Delta T}{dt} = \frac{dQ}{dT}\Delta T - \frac{dF}{dT}\Delta T + \Delta R \qquad (B6)$$

Upon rearranging Eq. (B6) and making use of the definition of λ, Eq. (19) results. This equation is of the form

$$\frac{d\Delta T}{dt} + a\Delta T = b \qquad (B7)$$

where $a = \lambda/I$ and $b = \Delta R/I$. Multiplication of Eq. (B7) by the integrating factor e^{at} and collapsing the resultant terms on the left hand side yields

$$\frac{d}{dt}(e^{at}\Delta T) = be^{at} \qquad (B8)$$

Integrating both sides of Eq. (B8) from time 0 to time t, dividing through by e^{at}, substituting for a and b, and noting that $\Delta T(0)=0$ (there is initially no temperature change) and $\Delta R/\lambda = \Delta T_{eq}$ (the equilibrium or steady-state temperature change), we obtain Eq. (20).

Box ends

Worksheet 6   Two-box, time-dependent climate model

Worksheet 5 indicates that, if the mixed layer were to be isolated from the deeper ocean, it would respond to changes in external heating with an e-folding time scale of 5-10 years, depending on the climate sensitivity. However, as soon as the mixed layer begins to warm, the heat flows between the mixed layer and deep ocean are altered, and this affects the subsequent warming of the mixed layer (and atmosphere). If the deep ocean is represented by a single well-mixed box with a given rate of mass exchange between the mixed layer and deep ocean boxes, then the temperatures of the two boxes will be the same in equilibrium. As the mixed layer warms in response to a positive radiative forcing, a heat flow from the mixed layer to the deep layer develops that depends on the temperature difference and the mass exchange rate. This slows the subsequent warming of the surface box. As heat flows into the deep box and it warms, the temperature difference between the two boxes – and the associated heat flux – gradually decreases, allowing a final warming of the surface box to the equilibrium value that is governed solely by the radiative damping to space.

The governing equations for the upper and lower boxes are

$$I_1 \frac{dT_1}{dt} = Q - F + \Delta R - F_d \qquad \qquad (25a)$$

and

$$I_2 \frac{dT_2}{dt} = F_d \qquad \qquad (25b)$$

where $I_2 = \rho c_p h_2$, h_2 is the thickness of the deep layer and F_d is the heat flux from the surface box to the deep box, given by

$$F_d = \kappa(T_1 - T_2) \qquad \qquad (26)$$

where $\kappa = \rho cp V/s$, V is the thickness of water in either box that exchanges mass with the other box every year and s is the number of seconds in a year. The default parameter values in the worksheet are $h_1 = 50$ m, $h_2 = 500$ m and $V = 7$ m/yr.

The transient responses of the surface layer and deep layer are illustrated in the figure embedded in Worksheet 6. The surface layer exhibits a rapid initial response, governed by the mixed layer thermal inertia, followed by a much slower response that is governed by the deep ocean mixed layer. The temperature response at which the transition occurs depends on the magnitude of V. During the second phase, the magnitude of the departure of the surface layer from its equilibrium response is directly proportion to T_1-T_2.

Worksheet 7   3-box terrestrial biosphere model

The terrestrial biosphere can be represented by a series of boxes representing different carbon reservoirs, such as woody tree parts, leafy tree parts, roots, above-ground detritus and different components of soil carbon. The terrestrial component of the carbon cycle is characterized by the amount of carbon in each reservoir, the rates of flow (fluxes) of carbon between the reservoirs, and the dependences of the fluxes on environmental variables such as temperature, soil moisture and atmospheric CO_2 concentration. Models that keep track of the nutrient content of different biomass fractions and of soil carbon can allow the rate of photosynthesis and of decomposition of detritus to depend on the nutrient content as well.

Here, a very simple 3-box representation of the global terrestrial biosphere will be used to represent basic modeling principles and some features of how simple models respond to temperature and CO_2 perturbations. The 3 boxes are: above-ground vegetation, detritus on the soil, and carbon in the soil. The assumed steady state carbon masses and fluxes, prior to any disturbances, are shown in **Figure 2.** This model is model 3 in Harvey (1989).
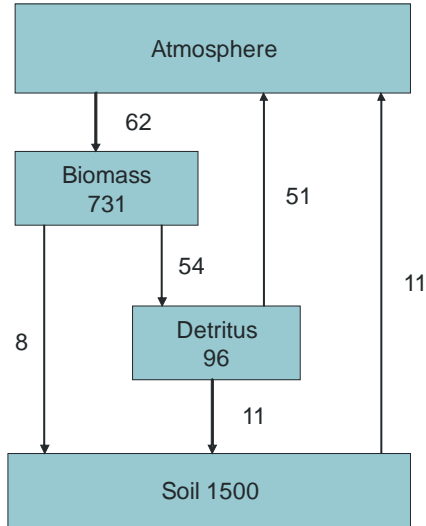
Figure 2. The structure of the terrestrial biosphere model of Worksheet 7. Numbers in boxes are the unperturbed amounts of carbon in Gt, while numbers next to arrows are annual fluxes (GtC/yr).

Intuitively, the rate of photosynthesis should depend on (among other things) the amount of biomass available to carry out photosynthesis. However, as the amount of biomass in a given area increases, effects of crowding will increase, eventually preventing any further increase in photosynthesis with increasing biomass. This behaviour can be represented by a logistic function, namely,

$$NPP = \upsilon B_1 - \rho B_1^2 \tag{27}$$

The flux out of box i and into box j is assumed to be proportional to the amount of biomass in box i times a coefficient α_{ij}. The governing equations for the amount of carbon in the boxes are thus

$$\frac{dB_1}{dt} = (\upsilon - \alpha_{12} - \alpha_{13})B_1 - \rho B_1^2 \tag{28}$$

$$\frac{dB_2}{dt} = \alpha_{12}B_1 - (\alpha_{23} + \alpha_{2a})B_2 \tag{29}$$

and

$$\frac{dB_3}{dt} = \alpha_{13}B_1 + \alpha_{23}B_2 - \alpha_{3a}B_3 \tag{30}$$

The α_{ij} coefficients are computed as

$$\alpha_{ij} = \frac{F_{ij}}{B_i} \tag{31}$$

where F_{ij} is the carbon flux from reservoir i to j, and the F_{ij} and B_i are taken from Figure 2.

The steady-state solution to Eq (28) (for which $dB_1/dt=0$) is

$$B_1 = \frac{\upsilon - \alpha_{12} - \alpha_{13}}{\rho} \tag{32}$$

We can incorporate the effects of changes in temperature and in atmospheric CO_2 concentration on the terrestrial biosphere through appropriate changes in the various coefficients. In general, increasing CO_2 concentration will increase the rate of photosynthesis, at least during the earlier stages of plant growth, but this initial effect increases at an ever slower rate as the CO_2 concentration increases. Increasing temperature will increase the rate of photosynthesis up to some optimal temperature, beyond which photosynthesis begins to decrease with increasing temperature. Here, we will adjust the coefficient governing photosynthesis during early growth stages, v, as follows:

$$\upsilon = \upsilon_o f_1(T) f_2(C) \tag{33}$$

where v_o is the initial value of v, C is CO_2 concentration,

$$f_1(T) = 1 + a_1 \Delta T + a_2 \Delta T^2 \tag{34}$$

and

$$f_2(C) = 1 + \beta \ln\left(\frac{C}{C_o}\right) \tag{35}$$

If v alone is increased in response to increasing CO_2 and temperature, the relative change in the steady state above-ground plant biomass (as given by Eq (32)) can be larger than the relative increase in v. However, numerous experimental and modeling studies indicate that the relative increase in steady state biomass B_1 is smaller than the relative increase in initial photosynthesis rates. Writing v as $v_o(1+\gamma)$, we shall assume that the steady state biomass B_1 increases by a factor $R_B=1+r\gamma$. Then, from Eq (32), the new ρ is given by

$$\rho = \frac{\upsilon_o(1+\gamma) - \alpha_{12} - \alpha_{13}}{R_B B_{1o}} \tag{36}$$

The coefficients governing respiration of detritus and soil carbon, α_{2a} and α_{3a}, are assumed to increase with temperature according to a Q_{10} relationship, namely,

$$\alpha_{ia} = (\alpha_{ia})_o Q_{10}^{\Delta T/10} \tag{37}$$

where $(\alpha_{ia})_o$ is the initial value of α_{ia} and Q_{10} is the factor by which α_{ia} increases for each 10 K warming.

The worksheet allows the user to specify the values of β, r and Q_{10} to be used in the 3-box model. Rather than specifying a and b, the relative enhancement in photosynthesis at a temperature increase of 2 K and the temperature increase at which the enhancement drops back to zero are specified by the user. The first part of the worksheet shows the resulting variation in $f_1(T)$ with T and of $f_2(C)$ with C.

The second part of the worksheet calculates the change in total carbon storage in the terrestrial biosphere due to concurrent increases in CO_2 and temperature. The worksheet gives a range in equivalent CO_2 concentration ranging from 280 ppmv (unperturbed, pre-industrial) to 840 ppmv (3 x pre-industrial). This along with the specified climate sensitivity allows determination of the equilibrium change in temperature. The user specifies the fraction of the equivalent CO_2 forcing that is due to CO_2 itself; only this portion stimulates photosynthesis. For a given set of carbon cycle feedback parameters (β, R_B, Q_{10}, a and b), the change in terrestrial carbon storage depends on the climate sensitivity and on the proportion of total radiative forcing that is due to increasing CO_2. A higher climate sensitivity or a smaller fraction of total forcing due to CO_2 means a larger temperature feedback on respiration relative to the CO_2 stimulation of photosynthesis, and a lower CO_2 concentration at which further increases in CO_2 tend to decrease photosynthesis.

The apparent feedback between temperature and carbon storage in the terrestrial biosphere is more complicated than in Worksheet 4, because now storage first increases (a negative feedback on atmospheric CO_2), then decreases (a positive feedback). This is illustrated in the figures that are embedded in Worksheet 7. Even more complex behaviour would be possible if coupling between the carbon and nitrogen cycles were added.

PART II: Emission and Climate Scenarios

Worksheet 8   Energy demand scenario generated from the Kaya identity

Energy demand is computed separately for OECD[a] and non-OECD countries in Worksheet 8 using the first three terms of the Kaya identity. The Kaya identity represents CO_2 emissions as the product of population, GDP (gross domestic product) per person, the amount of primary energy required on average per unit of GDP (the energy intensity), and the average carbon emission per unit of energy use (the carbon intensity). That is,

Emission (kgC) = P x ($/$P$) x (MJ/$) x (kgC/MJ)   (38)

The worksheet contains populations from the low and high scenarios (with slight modifications) in the 2008 edition of the United Nations Population Division's *World Population Prospects* (UNPD, 2008), summed over the specific countries that make up the OECD and non-OECD groups . The UNPD projections go to 2050 only, so they are extended beyond 2050 in the worksheet using the logistic growth function (derived in Box 2.1 of Harvey, 2010a), whereby the population $P(t)$ at some time t after 2050 is given by

---

[a] The OECD (Organization for Economic Cooperation and Development) consists of the following 30 so-called 'developed' countries: Australia, Austria, Belgium, Canada, Czech Republic, Denmark, Finland, France, Germany, Greece, Hungary, Iceland, Ireland, Italy, Japan, Korea, Luxembourg, Mexico, Netherlands, New Zealand, Norway, Poland, Portugal, Slovak Republic, Spain, Sweden, Switzerland, Turkey, United Kingdom, United States.

$$P(t) = \frac{P_U}{1 + ((P_U - P_o)/P_o)e^{-a(t-t_o)}} \tag{39}$$

where P_U is the assumed ultimate (and stable) population in each region, P_o is the population in 2050 according to the chosen UNPD scenario, and t_o=2050. As time progresses, P asymptotically approaches P_U with a time constant a. The user is invited to explore the impact of alternative values of P_U and the time constant for each region.

With regard to GDP/P in each region, values for 2005 are computed from the 2005 GDP and population in each region (GDP data are taken from the IMF World Economic Outlook Database, April 2009 Edition, available at http://www.imf.org/external/pubs/ft/weo/2009/01/weodata/index.aspx). For future GDP per person, Eq. (39) is used, this time with P_o representing GDP/P in 2005, P_U representing the assumed asymptotic GDP/P value, and t_o=2005. The initial GDP/P values are \$29866 and \$4398 in OECD and non-OECD countries, respectively, and the default asymptotic values are \$30,000 and \$25,000, respectively. The default time constants are 0.02/yr and 0.04/yr. As with population, the user is encourage to explore the ultimate impact on climatic change of alternative asymptotic values and time constants.

Finally, initial values of the energy intensity are computed from 2005 GDP and energy use data, the latter taken from Tables 2.1 and 2.2 of Harvey (2010a). The initial energy intensities are 6.9 MJ/\$ and 10.7 MJ/\$ averaged over OECD and non-OECD countries, respectively. These are assumed to decrease to default asymptotic values of 2.5 MJ/\$ in both regions using the logistic equation with time constants of 0.1/yr in both regions. These represent the effect of stringent implementation of all known energy efficiency measures over the next few decades, combined with some shift from heavy industry to services in non-OECD countries as economic wealth increases.

For the default parameter values given in the worksheet, global primary energy demand grows from 483 EJ/yr in 2005 to peak values of 599 EJ/yr in 2066 for the low population scenario and 846 EJ/yr in 2092 for the high population scenario. These relatively low projections of future energy demand are the result of the assumption of a very strong reduction in energy intensity (by factors of approximately 3 and 4 in OECD and non-OECD countries, respectively) over time. The user can, of course, explore the impact on energy demand (and, ultimately, on climate) of less stringent assumptions.

Worksheets 9 and 10   Energy supply scenario

The mix of energy supplies that meets the projected energy demand is computed as follows. First, the historical annual consumption of oil, natural gas and coal up to and including 2005 is specified based on CO_2 emission data from Marland et al (2008) combined with the appropriate emission factors. From 2006 onward, the potential consumption is computed based on the logistic function for cumulative consumption, namely,

$$C(t) = \frac{C_U}{1 + ((C_U - C_0)/C_0)e^{-a(t-t_o)}} \tag{40}$$

where $C(t)$ is the cumulative consumption up to and including year t, C_o is the cumulative consumption up to and including year t_o, and C_U is the ultimate cumulative consumption. The growth constant a is chosen such that the slope of $C(t)$ vs time is similar immediately before and after 2005 for each fossil fuel. The default values of C_U are twice, four times and almost four times the cumulative consumption up to 2005 for oil, natural gas and coal, respectively. A critical discussion of likely limits to the availability of these three resources can be found in Harvey (2010a, Chapter 2). Annual energy supply is given by the differences between $C(t)$ from one year to the next.

The logistic function is also used to directly project future annual supplies of three C-free energy sources. That is, Eq. (40) is used with $C(t)$ representing annual supply rather than cumulative consumption. The three C-free energy sources represented by Eq. (40) are hydro-electric energy, biomass, and "other" (which would include some combination of solar, wind, geothermal and oceanic energy). Energy supply in 2005 along with an ultimate rate of supply of energy and a time constant for approaching the ultimate rate are given in the worksheet and can be changed by the user. The technical feasibility and cost of supplying large amounts of energy from various C-free energy sources is comprehensively and critically discussed in Harvey (2010b).

As for nuclear energy, it is assumed in the worksheet that all nuclear reactors in existence in early 2010 are operated until the end of a 40-year operational lifespan and then retired without replacement. Data on the age distribution of existing nuclear reactors are provided in Worksheet 10 and used by Worksheet 9.

The total energy supply is compared with the energy demand and the surplus of energy supply over demand is given in column R (if demand exceeds supply, the surplus is negative). If there is a positive surplus, coal use is reduced (in column S). If the required coal supply drops to zero, any further excess of energy supply over demand is taken from the oil supply, and if oil supply can be reduced to zero, natural gas supply is reduced if needed. If fossil fuels have been completely eliminated, Biomass and 'Other' C-free energy supplies are reduced as needed so as to balance supply and demand. On the other hand, if energy demand exceeds total energy supply, then no adjustments are made (but alternative scenarios with more aggressive reductions in demand and/or a greater increase in C-free energy supply can be considered).

Worksheet 11 Interface with the Energy Demand Worksheets for *Energy and the New Reality*

The formulation of energy demand in Worksheet 8 is a simplification of the approach used in Harvey (2010a) which, together with Harvey (2010b), comprehensively and critically assesses what it would take to stabilize atmospheric CO_2 concentration at no greater than 450 ppmv. The Excel files used to generate the energy supply and demand scenarios, and the associated fossil fuel CO_2 emissions, are available online (at www.earthscan.co.uk/?tabid=102427). The calculation of energy demand in these files is more detailed than in Worksheet 8[b]. The fossil fuel

---

[b] In particular, separate fuel and electricity energy demands are projected separately in 10 different geopolitical regions based on changes in

- regional population,
- regional GDP per person per year,
- regional average activity per unit of GDP, and
- physical energy intensity per unit of activity.

CO_2 emissions that are produced from the Excel package can be pasted into Worksheet 11 and used in place of the fossil fuel CO_2 emissions from Worksheet 9. In this way, those who are so interested can explore the range of possible impacts on climatic change (as computed in Worksheets 13-17) resulting from very specific assumptions concerning future population, economic growth, activity levels and physical energy intensities at the regional level, and in the rate of deployment of C-free energy supplies at the global scale.

Worksheet 12 Impulse response for the absorption of emitted CO_2 by the oceans

Carbon dioxide continuously flows between the atmosphere and oceans as part of the natural carbon cycle. In an undisturbed, steady-state situation, the total flux of carbon from the atmosphere into the oceans is exactly balanced by the total flux out of the ocean (except for a small imbalance due to oxidation and outgassing of organic matter washed in by rivers). When additional CO_2 is added to the atmosphere (such as from human emissions), the extra CO_2 is removed by a variety of processes, some of which occur very rapidly (such as air-sea gas exchange occurring within months), while others (such as diffusive mixing into the deeper ocean) occur progressively more slowly. We can divide the pulse of CO_2 that is injected into the atmosphere into a series of fractions A_i, each of which decays (decreases in concentration) with its own time constant τ_i. The decrease in the amount of initially injected CO_2 that remains in the atmosphere is thus given by

$$G(t) = \sum_{i=1}^{n} A_i e^{-t/\tau_i} \qquad (41)$$

where $G(t)$ is the fraction of the initially injected CO_2 that remains after a time t, n is the number of terms (5 are used here) and $\sum A_i = 1.0$. $G(t)$ is the *impulse response* for CO_2.

A continuous emission of CO_2 can be represented by a series of annual emission pulses, each of which decays according to $G(t)$. The cumulative buildup of CO_2 at time t is the sum of the CO_2 remaining from all the emission pulses starting at time $t=0$ up to time t. A pulse that occurred at time t' occurred $t-t'$ years ago, so the amount of CO_2 remaining in the atmosphere from that pulse is $G(t-t')$. The amount of CO_2 in the atmosphere at time t is thus,

$$C(t) = C(0) + \int_{0}^{t} G(t - t') E(t') dt' \qquad (42)$$

where $E(t')$ is the rate of emission at time t'. The integral in Eq (42) is known as a *convolution integral*. The integral is evaluated numerically as

$$C(t_n) = C(t_o) + \sum_{i=i}^{i=n} E(t_i) G(t_n - t_i) \qquad (43)$$

Activity refers to such things as building floor area used per capita, distance travelled per year, freight movements per year, or tonnes of steel produced per year. Physical energy intensities refer to such things as energy used per unit of floor area or per tonne of steel produced. The energy intensities used in Worksheet 8, in contrast, are economic energy intensities (MJ per $ of GDP).

where $C(t_n)$ is the atmospheric CO_2 content at the end of year t_n, $E(t_i)$ is the total emission in year i and $G(t_n-t_i)$ is the amount of carbon emitted in year t_i that remains in the atmosphere at the end of year t_n.

Due to the non-linear carbon chemistry of ocean water, the rate of decay of successive pulses becomes slower as the cumulative emission (and hence, absorption by the oceans) increases. This can be represented by adjusting the coefficients in Eq. (41) as a function of the cumulative emission. Worksheet 12 contains the A_i and τ_i coefficients applicable prior to any human emissions and applicable to the next emission unit when the cumulative emissions reach 140 GtC, 560 GtC and 1680 GtC (the pre-industrial atmospheric CO_2 content was about 560 GtC). Columns B to E show the resulting impulse responses, while the figure embedded in the worksheet compares the 4 impulse responses graphically. The impulse response that is used is updated every 25 years based on the cumulative emissions up to the mid-point of the current 25-year block. The updated impulse response is used to compute the decay of all the annual emissions $E(t_i)$ occurring within the current 25-year time block. In order to illustrate the importance of the non-linear chemistry, CO_2 increases can be computed using both the initial impulse for all emissions and using the updated impulse responses. A control parameter in the worksheet determined which CO_2 concentration time series is used in subsequent calculations.

Worksheets 13, 14 and 15   Greenhouse gas concentrations

The concentration of CO_2 over time is computed in Worksheet 13 using the impulse responses from Worksheet 12 and the total emission, which consists of the following components:

- fossil fuel emissions,
- emissions from the chemical reactions that produce cement,
- emissions due to changes in land use,
- net emission due to the response of the terrestrial biosphere to increasing atmospheric CO_2 and changing temperature (this term is negative if the terrestrial biosphere exclusive of direct human alterations serves as a CO_2 sink),
- a source of CO_2 due to the decay of methane other than the decay of the natural, background sources of methane (so CO_2 from the decay of anthropogenic methane and of methane released from thawing permafrost soils is included), and
- a negative emission due to any sinks created through human intervention (this includes CO_2 directly captured from the air or captured from fossil fuel, biomass energy sources or the production of cement, or sinks created through reforestation, improved land management or buildup of biochar)

For the period 1850-2005, fossil fuel and cement-related CO_2 emissions from Marland et al (2008) are used. After 2005, fossil fuel emissions from Worksheet 9 or 11. The annual cement emissions after 2005 are assumed to rise to some peak in some peak year, then decline to some final value by 2100. The peak, peak year and long term value are all prescribed in Worksheet 13 by the user.

This worksheet also computes the buildup of methane (CH_4) and nitrous oxide (N_2O) due to emissions of these gases.

<u>Land use emissions</u>

The net emission due to land use changes involves direct emissions in any given year due to burning of biomass from land that is deforested, delayed decomposition of debris left on the land after deforestation, changes in the amount of carbon in the soil after deforestation, and absorption of CO_2 from the atmosphere due to regrowth forests on land that had been cleared and then later abandoned. Various estimates of regional and global emissions due to land use changes during the 1990s are summarized in Denman et al. (2007, Table 7.1). The estimated net emission due to land use change during the 1990s is 1.6±1.1 GtC/yr.

The buildup in atmospheric CO_2 depends on the fossil fuel and cement emissions (which are prescribed in the worksheet), the oceanic uptake (which is given by the impulse response in Worksheet 12), the response of the undisturbed terrestrial biosphere, and the uncertain net emissions due to land use changes. One option is to determine the net land use emissions such that the simulated increase in atmospheric CO_2 exactly matches observations. As long as the other emission sources are accurate and the response of the undisturbed biosphere is realistic, the deduced land use emissions should also be realistic (and the deduced emissions for the 1990s should fall within the 1.6±1.1 GtC/yr uncertainty range given above). Here, the net land use emissions as deduced in this way by Harvey (2001) are used here. These reach 1.5 GtC/yr by 1990, which gives an accurate buildup of atmospheric CO_2 for the default terrestrial biosphere feedback parameters (β, R_B, Q_{10}, a and b). The worksheet contains a parameter that allows the user to scale the history of land use emissions up or down, thereby permitting an accurate simulation of the observed CO_2 buildup when different biosphere feedback parameters are chosen.

Terrestrial biosphere source or sink

The sink or source of CO_2 due to CO_2 and temperature feedbacks with the terrestrial biosphere is computed using a 4-box terrestrial biosphere model in Worksheet 14, similar to that used in Worksheet 7 except that the above-ground biomass has been broken into separate woody and non-woody compartments, with the rate of photosynthesis dependent on the size of the non-woody compartment. Without this breakdown, the response of photosynthesis to short-term fluctuations in temperature (such as after volcanic eruptions) is unrealistically large. The long term response of the terrestrial biosphere to changing atmospheric CO_2 and temperature depends on the values chosen for the feedback parameters (β, R_B, Q_{10}, a and b). If the feedback parameters are chosen such that the terrestrial biosphere is a large CO_2 sink by the 1990s, then the land use emissions that are required in order to give the observed atmospheric CO_2 buildup will also be large. Conversely, if the feedback parameters are chosen such that the terrestrial biosphere is a small CO_2 sink by the 1990s, then the required land use emissions will be small. As noted above, the user is free to scale up or down an entire history of land use emissions when alternative values for the terrestrial biosphere feedback parameters are chosen, but the user should check that the resulting land use emissions during the 1990s fall within the estimated observational uncertainty range of 1.6±1.1 GtC/yr.

Yedoma soils

Worksheet 15 contains emission from a hypothetical feedback between warming and yedoma soils in Siberia. The yedoma soils are estimated to contain about 500 Gt of frozen carbon that is particularly susceptible to decomposition if it thaws. Khvorostyanov et al (2008) used a detailed permafrost model to simulate the impact of local warming on the yedoma soils, and they estimate that intense mobilization of carbon (2-3 GtC/yr) would begin when the regional warming reaches about 9ºC and continue for about 100 years. Inasmuch as the mean annual warming over land at the latitudes (60ºN to 70ºN) where yedoma soils occur is about twice the global mean warming (see

Figure 10.6 of Meehl et al, 2007), this implies that significant carbon release would occur in association with about 4.5°C global mean warming.

Emissions from yedoma soils are computed in Worksheet 15. The emission rate is assumed to increase linearly from 0 at some threshold global mean warming of ΔT_o to a value of F_1 at a warming of ΔT_1 and then to a larger value F_2 at a warming of ΔT_2. A fraction f_{CH4} of the emitted carbon is assumed to occur as CH_4 and the rest as CO_2. Emissions of CH_4 are of particular concern because the heat trapping of a CH_4 molecule is 26 times that of a CO_2 molecule, and because the methane buildup leads to an increase in its own lifespan in the atmosphere and to increases in tropospheric ozone and stratospheric water vapour, both of which add to the radiative forcing. The values of ΔT_o, ΔT_1, ΔT_2, F_1, F_2 and f_{CH4} can be chosen by the user, but should be constrained by the analysis in Khvorostyanov et al (2008) or in any subsequent work. Reasonable choices based on Khvorostyanov et al (2008) and the fact that some methane emissions from thawing permafrost regions already seem to be occurring (Walter et al., 2006) are $\Delta T_o = 0.8$ K, $\Delta T_o = 3.0$ K, $\Delta T_o = 4.5$ K, $F_1 = 0.2$-0.4 GtC/yr and $F_2 = 2$-3 GtC/yr and $f_{CH4} = 0.25$.

Methane and nitrous oxide concentrations

Worksheet 13 contains calculations for the buildup of CH_4 and N_2O in the atmosphere. Methane and nitrous oxide concentrations C in ppbv are governed by

$$\frac{dC}{dt} = rM - \tau C \tag{43}$$

where M is the annual emission rate in units of MtC/yr (CH_4) or MtN/yr (N_2O), r is a factor to convert from Mt to ppbv (equal to 0.469 ppbv/MtC for CH_4 and 0.201 ppbv/MtN for N_2O) and τ is the average molecular lifespan in years. The lifespan for N_2O is fixed at 120 years, but the lifespan of CH_4 depends on the CH_4 concentration itself according to the relationship

$$\tau = \tau_o \left(\frac{C}{C_o} \right)^{0.238} \tag{44}$$

where τ_o is the initial lifespan (8 years) and C_o is the initial concentration (693 ppbv). The emission M involves the background emission (184.7 MtC/yr, chosen so as to give the correct C_o when using τ_o), anthropogenic emissions and emissions from thawing of yedoma soils.

The lifespan of nitrous oxide is fixed, so only perturbations in nitrous oxide emissions (which are solely human emissions here) need be considered. The emission perturbation leads to a perturbation in concentration that can be directly added to the pre-industrial concentration and used to compute the radiative forcing due to the change in N_2O concentration.

Iterative solution procedure

The CO_2 emission or sink due to the terrestrial biosphere depends on the temperature and CO_2 increases, both of which depend in part on the terrestrial biosphere emission or sink. Similarly, the emissions of both CO_2 and CH_4 from thawing yedoma soils depend in part on the emissions themselves. Thus, an iterative procedure is required:

- When the 'Calculate CO_2 Increase' button is clicked after changing the emission scenario, climate sensitivity, or carbon cycle parameters, the CO_2 and temperature increases are computed based on the emissions due to the terrestrial biosphere feedback and thawing of yedoma soils as computed at the end of the previous set of iterations.
- The computed CO_2 and temperature increases lead to a new source or sink from the terrestrial biosphere and potentially from yedoma soils, but these will not affect the CO_2 concentration until the 'Calculate CO_2 Increase' button is clicked again
- Clicking the 'Calculate CO_2 Increase' button the second time changes the computed CO_2 and temperature increases and hence the computed yedoma and terrestrial biosphere source or sink, but the revised source/sink will not alter the computed CO_2 increase until the 'Calculate CO_2 Increase' button is clicked again.
- With each succession click of the 'Calculate CO_2 Increase' button, the change in the terrestrial biosphere and yedoma source/sink and hence in the CO_2 concentration and temperature will be smaller than with the previous click of the button, and after 5 to 7 clicks will be negligibly small.

Excel has some built-in capacity to carry out iterations (accessed by clicking on 'Tools', then 'Options', then going to the 'Calculation' sheet), but this is only a partial capacity. It is still necessary to click the 'Calculate CO_2 Increase' button 5-7 times whether the iteration limit is set to 1 or to 100. However, the calculations after a given click of the button take about 23 seconds when the iteration limit is set to 1 and 75 seconds with an iteration limit of 100, so the limit has been set to 1.

Worksheet 16 Greenhouse gas and other radiative forcings

The radiative forcings (W/m^2) due to the buildup of CO_2, CH_4 and N_2O are computed from

$$\Delta R_{CO2} = 3.75 \frac{\ln(C/C_o)}{\ln(2)} \tag{45}$$

$$\Delta R_{CH_4} = 0.036\left(\sqrt{C} - \sqrt{C_o}\right) - (CH_4 - N_2O)\_overlap\_term \tag{46}$$

and

$$\Delta R_{N_2O} = 0.14\left(\sqrt{C} - \sqrt{C_o}\right) - (N_2O - CH_4)\_overlap\_term \tag{47}$$

respectively, where C is the current concentration and C_o is the initial (pre-industrial) concentration (see Harvey et al., 1997).

The radiative forcing due to tropospheric ozone is computed as

$$\Delta R_{O_3} = \Delta R_{O_3-biomass}\left(\frac{E_{LU}(t)}{E_{LU}(2000)}\right) + \Delta R_{O_3-fossilfuel}\left(\frac{E_{FF}(t)}{E_{FF}(2000)}\right) + \Delta R_{O_3-CH_4}\left(\frac{\Delta C(t)}{\Delta C(2000)}\right) \tag{48}$$

where $\Delta R_{O3-biomass}$, $\Delta R_{O3-fossilfuel}$ and ΔR_{O3-CH4} are the radiative forcings in 2000 due to the increase in tropospheric ozone associated with biomass burning, fossil fuel use and the buildup of

atmospheric methane, respectively, $E_{LU}(t)$ and $E_{FF}(t)$ are the land use and fossil fuel CO_2 emissions in year t, respectively, and $\Delta C(t)$ is the increase in CH_4 concentration in year t from pre-industrial times. The total radiative forcing due to troposphere ozone is highly uncertain; the range given by Forster et al (2007) is 0.3-0.7 W/m^2 for 2005. The user can choose values of $\Delta R_{O3\text{-}biomass}$, $\Delta R_{O3\text{-}fossilfuel}$ and $\Delta R_{O3\text{-}CH4}$ such that the total lies within this range. The default values in the worksheet are 0.2 W/m^2 each.

The oxidation of methane in the stratosphere produces stratospheric water vapour. As this increase in water vapour is independent of changes in climate, it constitutes another radiative forcing (the increase in water vapour in the troposphere is driven by climatic warming itself and is thus an internal positive feedback rather than a forcing; it is accounted for in the prescribed climate sensitivity). This forcing is computed as

$$\Delta R_{strato-wv} = 0.00007\Delta C \tag{49}$$

where ΔC is the increase in methane concentration in ppbv since pre-industrial times.

A cooling effect due to sulphate aerosol emissions is also included. This radiative forcing involves two components: the reflection of sunlight in clear skies, which should roughly vary directly with the magnitude of aerosol emissions, and the increased reflectivity of clouds due to the role of aerosols as cloud condensation nuclei (CCN). Increasing aerosol concentration leads to a greater concentration of CCN, which in turn leads to more but smaller cloud droplets. As clouds consisting of smaller cloud droplets are more reflective, this is a cooling effect. The cloud cooling effect is expected to increase with the natural logarithm of the rate of aerosol emission. The default parameters in Worksheet 16 assign direct and indirect (cloud-related) cooling effects in 2000 of -0.25 W/m^2 and -0.55 W/m^2, respectively. Estimated historical sulphur emissions are used from 1950 to 2000 to compute the variation in radiative forcing up to 2000. Although the cooling effect of aerosols and the climate sensitivity are both highly uncertain, these two factors are not independent of one another. The climatic warming up to the present is proportional to the climate sensitivity times the net radiative forcing. As there is a fixed observed warming, a larger climate sensitivity requires a smaller net radiative forcing, and vice versa. A smaller net radiative forcing in turn requires a larger aerosol cooling offset. Thus, a larger climate sensitivity requires that the present cooling affect due to anthropogenic (human-caused) aerosols also be larger, and vice versa. The user can experiment with different combination of climate sensitivity and aerosol forcing in 2000, but other constraints indicate that the aerosol forcing should not be more than half of the GHG heating (see Harvey and Kaufmann, 2002).

After 2000, sulphur emissions are given by

$$E_{aerosol}(t) = E_{aerosol}(2000)\left(\frac{E_{ff}(t)}{E_{ff}(2000)}\right)R_{SC} \tag{50}$$

where $E_{aerosol}(t)$ is the emission of aerosol precursors in year t, $E_{ff}(t)$ is the fossil fuel CO_2 emission in year t, and R_{SC} is a factor equal to 1.0 up to 2010 and given by

$$R_{SC} = R_{SC-final} + (1 - R_{SC-final})e^{-(t-2010)/\tau} \tag{51}$$

after 2000, where $R_{SC\text{-}final}$ is the final value of R_{SC} and τ is a time constant for approaching R_{SC}. The default values of these two parameters are 0.25 and 10 years, respectively. A declining RSC

value accounts for the likelihood that concerns over acid rain (which are associated with S and N aerosols) will likely lead to increasingly stringent controls on S and N emissions, even if there are no restrictions on CO_2 emissions. This in turn will tend to accelerate the warming as the cooling effect of aerosols weaken. If fossil fuel emissions are falling, aerosol emissions and the associated cooling effect will also weaken, causing a short term acceleration in warming even as CO_2 emissions are reduced. The user can explore these relationships by altering the emission scenario and aerosol parameters.

The final two forcings considered are those due to volcanic eruptions and solar variability over the period 1850-2000. These are taken from Harvey and Kaufmann (2002). Future volcanic eruptions of course cannot be predicted and so are left out, while the solar forcing after 2000 is assumed to be constant at the year-2000 value.

A separate Excel sheet contains figures showing the various forcings.

Worksheet 17   Climate model response

The 2-box climate model presented in Worksheet 6 is used to compute the variation in surface temperature in response to all of the forcings described for Worksheet 16.

Worksheet 18   Climate and carbon cycle model diagnostics

The final worksheet presents two sets of model diagnostics, one based on conservation of energy and the other based on conservation of mass.

Note the following energy balance relationships:

Radiative forcing – radiative damping = net radiation
Radiative forcing – radiative damping – damping to ocean = energy balance of box 1
Energy balance of box 2 = damping to ocean
Net radiation = energy balance of box 1 + energy balance of box 2
The temperature of either box increases only when the energy balance for that box is positive, and can initially continue to increase after GHG concentrations begin to fall.

Note the following carbon balance relationships:

Atmospheric increase = total emissions – total sinks
Atmospheric CO_2 can be increasing even while emissions are falling, as long as sources (emissions) exceed sinks.

References

Bony, S. et al. (2006) How well do we understand and evaluate climate change feedback processes? *Journal of Climate*, **19**, 3445-3482.

Denman, K.L. et al. (2007) Couplings between changes in the climate system and biogeochemistry, in *Climate Change 2007: The Physical Science Basis. Contribution of Working Group I to the Fourth Assessment Report of the Intergovernmental Panel on Climate Change* (S. Solomon, D. Qin, M. Manning, Z. Chen, M. Marquis, K.B. Averyt, M. Tignor and H.L. Miller (eds.)), Cambridge University Press, Cambridge, UK and New York NY, USA

Forster, P. et al. (2007) 'Changes in atmospheric constituents and in radiative forcing', in S. Solomon, D. Qin, M. Manning, Z. Chen, M. Marquis, K. B. Averyt, M. Tignor and H. L. Miller (eds) *Climate Change 2007: The Physical Science Basis, Contribution of Working Group I to the Fourth Assessment Report of the Intergovernmental Panel on Climate Change*, Cambridge University Press, Cambridge and New York, pp129-234

Harvey, L.D.D. (1989) Effect of model structure on the response of terrestrial biosphere models to CO_2 and temperature increases, *Global Biogeochemical Cycles*, **3**, 137-153.

Harvey, L.D.D. (2000) *Global Warming: The Hard Science,* Prentice Hall, Harlow, 336 pages*.*

Harvey, L.D.D. (2001) A quasi-one-dimensional coupled climate-carbon cycle model, Part II: The carbon cycle component, *Journal of Geophysical Research – Oceans* **106 (C10),** 22355-22372.

Harvey, L.D.D. (2010a) *Energy and the New Reality, Volume 1: Energy Efficiency and the Demand for Energy Services*. Earthscan, London, 614 pages.

Harvey, L.D.D. (2010b) *Energy and the New Reality, Volume 2: C-Free Energy Supply*. Earthscan, London, 565 pages.

Harvey, L.D.D., Gregory, J., Hoffert, M., Jain, A., Lal, M., Leemans, R., Raper, S., Wigley, T. and de Wolde, J. (1997) *An Introduction to Simple Climate Models used in the IPCC Second Assessment Report*, Intergovernmental Panel on Climate Change,

Harvey, L.D.D. and Kaufmann, R. (2002) Simultaneously constraining climate sensitivity and aerosol radiative forcing, *Journal of Climate* **15**, 2837-2861.

Khvorostyanov, D. V., Ciais, P., Krinner, G. and Zimov, S. A. (2008) 'Vulnerability of east Siberia's frozen carbon stores to future warming', *Geophysical Research Letters*, vol 35, L10703, doi:10.1029/2008GL033639

Marland, G., Boden, T. A. and Andres, R. J. (2008) 'Global CO_2 emissions from fossil fuel burning, cement manufacture, and gas flaring, 1751–2005', Carbon Dioxide Information and Analysis Centre, Oak Ridge, www.cdiac.esd.ornl.gov/trends/emis/meth_reg.htm

Plattner, G/-K. and Co-authors (2008) Long-term climate commitments projected with climate-carbon cycle models, *Journal of Climate*, **21,** 2721-2751.

Ringer, M.A. et al (2006) Global mean cloud feedbacks in idealized climate change experiments, *Geophysical Research Letters,* **33**, L07718, doi:10.1029/2005GL025370.

Schlesinger, M.E. (1985) Appendix A: Analysis of results from energy balance and radiative convective models, in MacCracken, M.C. and Luther, F.M. (eds.), *Projecting the Climatic Effects of Increasing Carbon Dioxide*, U.S. Department of Energy, DOE/ER-0237, pp. 281-319.

Thompson, S.L. and Schneider, S.H. (1979) A seasonal zonal energy balance climate model with an interactive lower layer, *Journal of Geophysical Research*, **84**, 2401-2414.

Walter, K.M., Zimov, S.A., Chanton, J.P., Verbyla, D. and Chapin III, F.S. (2006) Methane bubbling from Siberian thaw lakes as a positive feedback to climate warming, *Nature***, 443**, 71-75

Warren, S.G. and Schneider, S.H. (1979) Seasonal simulation as a test for uncertainties in the parameterization of a Budyko-Sellers zonal climate model, *Journal of the Atmospheric Sciences*, **36**, 1377-1391.